2018

Inhibition of human N- and T-type calcium channels by an ortho-phenoxyanilide derivative, MONIRO-1

Jeffrey R. McArthur
University of Wollongong, RMIT University, jeffreym@uow.edu.au

Leonid Motin
University of Wollongong, RMIT University

Ellen Gleeson
CSIRO Manufacturing, Monash University

Sandro Spiller
Monash University

Richard J. Lewis
University of Queensland

See next page for additional authors

Publication Details

McArthur, J. R., Motin, L., Gleeson, E. C., Spiller, S., Lewis, R. J., Duggan, P. J., Tuck, K. L. & Adams, D. J. (2018). Inhibition of human N- and T-type calcium channels by an ortho-phenoxyanilide derivative, MONIRO-1. British Journal of Pharmacology, 175 (12), 2284-2295.

Inhibition of human N- and T-type calcium channels by an ortho-phenoxyanilide derivative, MONIRO-1

Abstract

Background and Purpose: Voltage-gated calcium channels are involved in nociception in the CNS and in the periphery. N-type ($Ca_v2.2$) and T-type ($Ca_v3.1$, $Ca_v3.2$ and $Ca_v3.3$) voltage-gated calcium channels are particularly important in studying and treating pain and epilepsy. **Experimental Approach**: In this study, whole-cell patch clamp electrophysiology was used to assess the potency and mechanism of action of a novel ortho-phenoxylanilide derivative, MONIRO-1, against a panel of voltage-gated calcium channels including $Ca_v1.2$, $Ca_v1.3$, $Ca_v2.1$, $Ca_v2.2$, $Ca_v2.3$, $Ca_v3.1$, $Ca_v3.2$ and $Ca_v3.3$. **Key Results**: MONIRO-1 was 5- to 20-fold more potent at inhibiting human T-type calcium channels, $hCa_v3.1$, $hCa_v3.2$ and $hCa_v3.3$ (IC_{50} : 3.3 ± 0.3, 1.7 ± 0.1 and 7.2 ± 0.3 μM, respectively) than N-type calcium channel, $hCa_v2.2$ (IC_{50} : 34.0 ± 3.6 μM). It interacted with L-type calcium channels $Ca_v1.2$ and $Ca_v1.3$ with significantly lower potency (IC_{50} > 100 μM) and did not inhibit $hCa_v2.1$ or $hCa_v2.3$ channels at concentrations as high as 100 μM. State- and use-dependent inhibition of $hCa_v2.2$ channels was observed, whereas stronger inhibition occurred at high stimulation frequencies for $hCa_v3.1$ channels suggesting a different mode of action between these two channels. **Conclusions and Implications**: Selectivity, potency, reversibility and multi-modal effects distinguish MONIRO-1 from other low MW inhibitors acting on Ca v channels involved in pain and/or epilepsy pathways. High-frequency firing increased the affinity for MONIRO-1 for both $hCa_v2.2$ and $hCa_v3.1$ channels. Such Ca_v channel modulators have potential clinical use in the treatment of epilepsies, neuropathic pain and other nociceptive pathophysiologies.

Disciplines

Medicine and Health Sciences

Publication Details

McArthur, J. R., Motin, L., Gleeson, E. C., Spiller, S., Lewis, R. J., Duggan, P. J., Tuck, K. L. & Adams, D. J. (2018). Inhibition of human N- and T-type calcium channels by an ortho-phenoxyanilide derivative, MONIRO-1. British Journal of Pharmacology, 175 (12), 2284-2295.

Authors

Jeffrey R. McArthur, Leonid Motin, Ellen Gleeson, Sandro Spiller, Richard J. Lewis, Peter J. Duggan, Kellie L. Tuck, and David J. Adams

Inhibition of human N- and T-type calcium channels by an ortho-phenoxyanilide derivative, MONIRO-1

Running title: MONIRO-1 block of voltage-gated calcium channels

Jeffrey R McArthur,[ab1] Leonid Motin,[ab1] Ellen C Gleeson,[c,d] Sandro Spiller,[d] Richard J Lewis,[e] Peter J Duggan,[c,f], Kellie L Tuck[d] and David J Adams[ab1]*

[a]Illawarra Health and Medical Research Institute, University of Wollongong, Wollongong NSW 2522, Australia.
[b]Health Innovations Research Institute, RMIT University, Melbourne VIC 3083, Australia.
[c]CSIRO Manufacturing, Bag 10, Clayton South VIC 3169, Australia.
[d]School of Chemistry, Monash University, Clayton VIC 3800, Australia.
[e]Institute for Molecular Bioscience, The University of Queensland, St Lucia QLD 4072, Australia.
[f]School of Chemical and Physical Sciences, Flinders University, Adelaide SA 5042, Australia.

[1]Present address: Illawarra Health and Medical Research Institute (IHMRI), University of Wollongong, Wollongong NSW 2522, Australia.

*Authors for correspondence:
David J. Adams, Illawara Health and Medical Research Institute (IHMRI), University of Wollongong, Wollongong NSW 2522, Australia. Tel: +61 2 4239 2264 Email: djadams@uow.edu.au

BACKGROUND AND PURPOSE
Voltage-gated calcium channels are involved in peripheral and central nervous system nociception. N-type ($Ca_v2.2$) and T-type ($Ca_v3.1$, Ca_v 3.2 and Ca_v 3.3) voltage-gated calcium channels are particularly important in studying and treating pain and epilepsy.

EXPERIMENTAL APPROACH
In this study, whole-cell patch clamp electrophysiology was used to assess the potency and mechanism of action of a novel *ortho*-phenoxylanilide derivative, MONIRO-1, against a panel of voltage-gated calcium channels including $Ca_v1.2$, $Ca_v1.3$, $Ca_v2.1$, $Ca_v2.2$, $Ca_v2.3$, $Ca_v3.1$, $Ca_v3.2$ and $Ca_v3.3$.

KEY RESULTS
MONIRO-1 was 5-20-fold more potent at inhibiting human T-type calcium channels, $hCa_v3.1$, $hCa_v3.2$ and $hCa_v3.3$ (IC_{50}: 3.3 ± 0.3 μM, 1.7 ± 0.1 μM and 7.2 ± 0.3 μM, respectively) than N-type calcium channel, $hCa_v2.2$ (IC_{50}: 34.0 ± 3.6 μM). It interacts with L-type calcium channels $Ca_v1.2$ and $Ca_v1.3$ with significantly lower potency (IC_{50} >100 μM), and does not inhibit $hCa_v2.1$ or $hCa_v2.3$ at concentrations as high as 100 μM. Interestingly, state- and use-dependent inhibition of $hCa_v2.2$ was observed, whereas stronger inhibition occurred at high stimulation frequencies for $hCa_v3.1$ suggesting a different mode of action between these two channels.

CONCLUSIONS AND IMPLICATIONS
Selectivity, potency, reversibility and multi-modal effects distinguish MONIRO-1 from other small molecule inhibitors acting on Ca_v channels involved in pain and/or epilepsy pathways. For both $hCa_v2.2$ and $hCa_v3.1$, high frequency firing increases the affinity for MONIRO-1 for both channels. Such Ca_v channel modulators have potential clinical use in the treatment of epilepsies, neuropathic pain and other nociceptive patho-physiologies.

KEYWORDS

Electrophysiology; Neuronal Ca_v channels; State-dependent block; Human embryonic kidney cells; Pain; Epilepsy

ABBREVIATIONS

hERG, human Ether à-go-go Related Gene; SSI, steady-state inactivation; VGCCs, voltage-gated calcium channels.

INTRODUCTION

Sensory nerve conduction relies on the coordinated activation of a suite of ion channels to generate fast and accurate responses to mechanical, thermal and chemical stimuli. In the periphery, harmful signals are perceived by 'nociceptive' neurons and relayed centrally via voltage-activated ion channels (K_v, Na_v, Ca_v) and ligand-gated ion channels (TRP, K2P, P2X) (Waxman et al., 2014) as part of the 'pain-signalling cascade' (Gold et al., 2010). In chronic pain, these pathways are characterized by hyperactivity (Waxman et al., 2014) and the effects of noxious stimuli are enhanced (hyperalgesia) to the point where non-noxious stimuli are painful (allodynia) (see recent review by Guo and Hu (Guo et al., 2014)). Voltage-gated calcium channels (VGCCs) involved in pain pathways are localized to dendrites of primary sensory neurons and contribute to integrate nociceptive stimuli at the spine by regulating the release of pro-nociceptive neurotransmitters, including substance P, calcitonin gene-related peptide and glutamate, at the presynaptic nerve terminus (Simms et al., 2014). Therefore, modulating specific Ca_v subtypes could be a promising way to treat chronic pain.

Five distinct voltage-gated calcium current types have been described in mammalian cells: L- ($Ca_v1.1$-1.4), P/Q- ($Ca_v2.1$), N- ($Ca_v2.2$), R- ($Ca_v2.3$) and T- ($Ca_v3.1$-3.3) types (Catterall et al., 2005). Importantly, each Ca_v subtype has distinct electrophysiological properties, tissue-specific localization and pharmacological profiles (Catterall et al., 2005). N-type calcium channels have been a major focus of research because they are localized at the presynaptic terminals of sensory nerves in the dorsal horn of the spinal cord, where they play a critical role in pain signalling (Lee, 2014; Saegusa et al., 2001). As a result, $Ca_v2.2$ channels are strongly implicated in a range of chronic pain conditions including neuropathic pain (pain caused by injury to the nervous system). Specific $Ca_v2.2$ channel inhibitors have clinical applications (Altier et al., 2004; Bourinet et al., 2014; Perret et al., 2009), such as ω-conotoxin MVIIA (Ziconotide). Ziconotide selectively targets $Ca_v2.2$ channels and is used to effectively treat intractable chronic pain conditions (Pope et al., 2013). However, due to its chemical nature, Ziconotide must be administered into the cerebrospinal fluid via the intrathecal route and has a relatively narrow therapeutic window (Pope et al., 2013).

T-type calcium channels modulate neuronal excitability in the peripheral and central nervous systems, where they are linked to hyperexcitable states such as epilepsy, pain and tremor disorders like Parkinson's disease (Bourinet et al., 2005; Choi et al., 2007; Kim et al., 2001). Previously characterized T-type calcium channels inhibitors, such as mibefradil and ethoximide, have analgesic properties, suggesting that T-type channels may be involved in pain signalling (Flatters et al., 2004; Matthews et al., 2001; Todorovic et al., 2002; Wen et al., 2010). Unfortunately, mibefradil and ethoximide target a wide range of voltage-gated ion channels, including sodium, potassium and chloride channels (Chouabe et al., 1998; Eller et al., 2000; Nilius et al., 1998).

To overcome this lack of specificity, small molecule T-type calcium channel inhibitors were designed and have been shown to provide analgesic effects in mouse models of inflammatory and neuropathic pain (Bladen et al., 2015; Kraus et al., 2010; Reger et al., 2011). Of particular note is the analgesic, small molecule TTA-A2, which is more potent against inactivated than closed or resting channels (IC_{50} values of 100 nM and 10 μM at $Ca_v3.1$, respectively), indicating its effects on targets are state-dependent (Francois et al., 2013). Based on these findings, N- and T-type calcium channels are of particular interest for the study and treatment of pain (see recent reviews by (Cheong et al., 2013; François et al., 2014; Lee, 2014; Lee, 2013; Sekiguchi et al., 2013; Simms et al., 2014).

During the last five years, numerous reports have described small molecule $Ca_v2.2$ channel inhibitors as alternatives to Ziconotide (see review by Lee (Lee, 2014)). Regrettably, clinical development of the most promising of these small-molecules, Z160, a reformulated form of NP118809 (Zamponi et al., 2009) (compound **1**, Fig. 1), was discontinued after it failed to meet end points in phase II clinical trials (Eller et al., 2000). Due to this and the need for effective and safe therapeutics for chronic pain, the development of new classes of small-molecule Ca_v channel antagonists is of significant interest.

The pharmacophore of $Ca_v2.2$-selective ω-conotoxin GVIA (Andersson et al., 2009; Baell et al., 2004; Baell et al., 2006; Duggan et al., 2009; McCleskey et al., 1987) has been carefully studied and has led to the identification of a series of compounds that block $Ca_v2.2$ channels in a concentration-dependent manner (Tranberg et al., 2012).

We focused on developing low molecular weight calcium channel inhibitors with enhanced biophysical properties including reversibility, voltage- and/or state-dependence. Compounds acting via these mechanisms can strongly inhibit channels upon membrane depolarization (Butterworth et al., 1990; Hondeghem et al., 1984) by preferentially targeting the open and/or inactivated states over the resting state. Such compounds would facilitate inhibition of high-frequency firing or depolarised nerves that can predominate in chronic pain states, and could act within a wider therapeutic window.

To develop these calcium channel inhibitors, we screened a small library of related derivatives, using FLIPR Tetra® high-throughput cellular screening system, for their ability to inhibit $Ca_v2.2$-mediated calcium responses in SH-SY5Y cells using the fluorescent indicator Calcium 4 dye (Molecular Devices, Sunnycale, CA, USA) (Gleeson et al., 2015). In this assay, MONIRO-1 inhibited Ca^{2+} responses elicited by KCl-mediated depolarization with an IC_{50} of 124 μM. Subsequently, we characterized the *ortho*-phenoxyanilide derivative MONIRO-1 (Compound **2**, Fig. 1) electrophysiologically. To directly assess the biophysical properties of MONIRO-1 inhibition of voltage-gated calcium channels, we used the whole-cell patch clamp recording technique to study a comprehensive array of Ca_v channels heterologously or stably expressed in HEK-293 cells. MONIRO-1 was 5−100 times more potent against T-type calcium channels ($Ca_v3.1$, $Ca_v3.2$ and $Ca_v3.3$) than N-type ($Ca_v2.2$) and L-type ($Ca_v1.2$ and $Ca_v1.3$) channels. No inhibition of P/Q ($Ca_v2.1$) or R-type currents ($Ca_v2.3$) was detected in the presence of up to 100 μM MONIRO-1. Furthermore, MONIRO-1 modulated $Ca_v2.2$ differently at various stimulation rates and in a state-dependent fashion, preferentially inhibiting hyperactive channels such as those likely to predominate in pathologically augmented pain states.

1. METHODS

1.1 Chemical synthesis.

Compound **2**, *N*-(2-(4-fluorophenoxy)phenyl)-4-(3-guanidinopropoxy)benzamide hydrochloride, MONIRO-1, was synthesized from 2-(4-fluorophenoxy)aniline in four steps, as reported previously (Gleeson et al., 2015). ^{1}H NMR (400 MHz, CD_3OD): δ 7.88-7.85 (m, 1H), 7.78-7.76 (m, 2H), 7.21-7.18 (m, 2H), 7.07-6.98 (m, 6H), 6.97-6.94 (m, 1H), 4.13 (t, J = 5.9 Hz, 2H), 3.41 (t, J = 6.8 Hz, 2H), 2.11-2.05 (m, 2H). ^{13}C

NMR (100 MHz, CD_3OD): δ 168.2, 163.2, 160.2 (d, *J* = 239 Hz), 158.7, 154.4, 151.0, 130.5, 130.4, 127.9, 127.6, 126.9, 125.0, 120.8 (d, *J* = 8.3 Hz), 120.1, 117.2 (d, *J* = 23.4 Hz), 115.4, 66.3, 39.5, 29.5. ^{19}F NMR (376 MHz, CD_3OD): δ -120.6, purity > 92%, determined by HPLC analysis (λ = 254 nm), all tests were performed using the same batch of compound. The positive control, compound **1** (Z160/NP118809) (Zamponi et al., 2009; Zikolova et al., 1972), was prepared by *N*-(3-dimethylaminopropyl)-*N′*-ethylcarbodiimide-assisted acylation of *N*-benzhydryl piperazine with 3,3-diphenylpropanoic acid. Control compound NNC 55-0396 dihydrochloride was provided by Alomone Labs (Jerusalem, Israel).

1.2 Cell culture and transfection.

HEK293 cells containing the SV40 Large T-antigen (HEK293T) were cultured at 37 °C, 5% CO_2 in Dulbecco's Modified Eagle's Medium (Invitrogen Life Technologies, Australia) supplemented with 10% fetal bovine serum (Invitrogen), 1% penicillin and streptomycin (Invitrogen). HEK293T cells stably expressing the human $Ca_v2.1$ (P/Q-type) calcium channel (α_{1A-2} splice variant; GenBank accession no. AF004883.1), $Ca_v2.2$ (N-type) calcium channel (transcript variant 1, NM_000718) or $Ca_v2.3$ (R-type) calcium channel (neuronal α_{1E-3} splice variant, also called α_{1E-c}, L29385.1) were obtained from Merck and cultured according to procedures described by Dai *et al.* (Dai et al., 2008). These cell lines co-express recombinant human Ca_v $\alpha_{2b}\delta$-1 (M76559.1) and Ca_v β_{3a} (NM_000725) auxiliary subunits (Dai et al., 2008). Cells are plated onto 12 mm cover glass and incubated at 30 °C, 5% CO_2 for 24-48 hours prior to recording.

In a separate series of experiments, HEK293T cells were transiently co-transfected with plasmid cDNAs encoding human $Ca_v1.3$ (provided by Dr G. Zamponi, University of Calgary) with $\alpha_2\delta$-1 and β_3, $Ca_v3.1$ (provided by Dr G. Zamponi), human $Ca_v3.2$ (CACNA1HB; Origene Technologies, Rockville, MD), human $Ca_v3.3$ a1Ic-HE3-pcDNA3 was a gift from Edward Perez-Reyes(Gomora et al., 2002) (Addgene plasmid # 45810) and $K_v11.1$ (hERG) (provided by Dr J. Vandenberg, Victor Chang Cardiac Research Institute, Sydney). After transfection, cells were plated on glass coverslips and incubated at 37 °C, 5% CO_2 overnight. The transfection medium was then replaced with culture medium and cells were incubated at 30 °C, 5% CO_2.

1.3 Electrophysiology.

Electrophysiological experiments were carried out 1-3 days after transfection using the whole-cell patch clamp recording technique. Cells were superfused with a solution containing 110 mM NaCl, 10 mM $CaCl_2$, 1 mM $MgCl_2$, 5 mM CsCl, 30 mM TEA-Cl, 10 mM d-glucose and 10 mM HEPES, pH 7.4 with TEA-OH (~310 mOsmol/kg). Fire-polished borosilicate patch pipettes with tip-resistance values of 1–3 MΩ were filled with an intracellular solution containing 125 mM Kgluconate, 5 mM NaCl, 2 mM $MgCl_2$, 5 mM EGTA, 4 mM MgATP and 10 mM HEPES, pH 7.2 with CsOH (~300 mOsmol/kg). Depolarization-activated calcium currents were recorded at room temperature (21-23 °C) using a Multiclamp 700B patch clamp amplifier (Molecular Devices, Sunnyvale, CA) controlled by DigiData 1322/Clampex 9.2 acquisition systems. MONIRO-1 stock solution was dissolved in 5% DMSO to a concentration of 5 mM. MONIRO-1 was further diluted in recording solution to appropriate concentrations. Previous experiments using the maximal concentration of DMSO used, 0.1% at 100 µM, did not modulate VGCC currents in recording solution.

Depolarization-activated calcium currents (I_{Ca}) were evoked from a holding potential of −80 mV, with a 135 ms (50 ms for T-type) voltage step to a test potential (determined from peak of I-V curve) applied every 10 s. When evaluating I_{Ca} amplitude in the presence and absence of various compounds, test depolarizations of varying durations were applied at a frequency of 0.03–2 Hz, from a holding potential of −60, −80 or −100 mV to a test potential determined from an I-V relationship to elicit peak inward current. To examine the effects of pulse duration on MONIRO-1 block and recovery from block, pulses of either 45 or 135 ms for $Ca_v2.2$ (30 µM) or 15 or 50 ms for $Ca_v3.1$ (3 µM) were elicited at a frequency of 0.1 Hz ($V_h = -80$ mV). Similarly, to study the frequency dependence of MONIRO-1 inhibition, test pulses (45 ms for $Ca_v2.2$ or 15 ms for $Ca_v3.1$) were elicited at rates of 0.03, 0.1 and 0.2 Hz for $Ca_v2.2$ (10 µM MONIRO-1) and 0.03, 0.1, 0.2, 1 and 2 Hz for $Ca_v3.1$ (3 µM MONIRO-1). To determine the time constants for activation and inactivation of macroscopic currents, we used a single exponential equation to fit the traces in control and after MONIRO-1 application.

Activation curves were measured from test pulses from -80 to +80 mV every 5 mV for $Ca_v2.2$ and $Ca_v3.1$ channels ($V_h = -80$ mV) before and after MONIRO-1 application. Steady-state inactivation (SSI) curves were generated from various pre-

pulse potentials (−120 to 0 mV for $Ca_v2.2$; −85 to −20 mV for $Ca_v3.1$) of 10 s ($Ca_v2.2$) or 1 s ($Ca_v3.1$). Recovery from inactivation was examined using a double-pulse protocol, varying the time between a fully inactivating prepulse and the test pulse repeated every 15 s, using a concentration of MONIRO-1 which inhibits ~50% of the current. Recovery data was best fit by a double exponential. Currents were filtered at 3 kHz and sampled at 10 kHz. Leak and capacitive currents were subtracted using a −P/4 pulse protocol. Data were stored digitally on a computer for further analysis.

1.3 Data analysis.

Data analysis and graphs were built using OriginPro (Origin Lab Corporation, North Hampton, MA, USA). Concentration-response curves were generated by plotting current in the presence of MONIRO-1 ($I_{compound}$) over current prior to application ($I_{control}$) versus a range of MONIRO-1 concentrations tested. Typically, 4-6 concentrations per channel were screened with 5-9 cells per concentration. Concentration-response data was plotted using a rectangular hyperbola assuming a Hill coefficient of 1, using the following expression,

$(I_{compound}/I_{control}) = 1/(1+IC_{50}/[drug])$,

where IC_{50} is the concentration at which half-maximal inhibition was observed.

Steady-state activation and inactivation curves were generated using a modified Boltzmann equation,

$G = 1/(1+\exp((Vm-V_{0.5})/\kappa a))$,

where V_m is the test potential, $V_{0.5}$ is the half-maximal activation potential and κa is the slope factor. SSA and SSI data were each recorded from 5-7 individual experiments per channel examined. Recovery from inactivation curves were the results from 5-6 independent experiments where the complete set of recovery from inactivation time points were acquired. The data was fit using a double exponential of the following equation,

$I = 1+A_{fast} *\exp(-t/\tau_{fast}) + A_{slow} *\exp(-t/\tau_{slow})$,

where τ is the fast and slow time constant, t is the recovery time and A is the amplitude of the fast and slow time constants. Statistical significance of $P < 0.05$ was determined using unpaired Student's t-tests or one-way ANOVA using Tukey post hoc test. All data reported as mean ± standard error.

2. RESULTS

3.1 Selective inhibition of human N- and T-type calcium channel subtypes.

Whole-cell calcium currents were elicited by depolarizing pulses at a frequency of 0.1 Hz from a holding potential of −80 mV. MONIRO-1 reversibly inhibited channel currents mediated by $Ca_v3.2$ (IC_{50} 1.7 ± 0.1 μM, n = 5-9 cells/concentration), $Ca_v3.1$ (IC_{50} 3.3 ± 0.3 μM, n = 5-6 cells/concentration), $Ca_v3.3$ (IC_{50} 7.2 ± 0.3 μM, n = 5 cells/concentration) and $Ca_v2.2$ (IC_{50} 34.0 ± 3.6 μM, n = 5-7 cells/concentration) (Fig. 2 and 3A). The effects of MONIRO-1 were further investigated on a panel of VGCCs. At 100 μM, MONIRO-1 had no apparent effect on $Ca_v2.1$ (n = 5) or $Ca_v2.3$ (n = 5) (Fig. 3B), but inhibited $Ca_v1.2$ and $Ca_v1.3$-mediated currents by 45.8 ± 0.9% (n = 5) and 27.0 ± 1.2% (n = 5), respectively.

In comparison, Z160/NP118809 (Zamponi et al., 2009) inhibited $Ca_v2.2$-mediated currents with an IC_{50} of 0.28 ± 0.02 μM (n = 5-6 cells/concentration), without affecting $Ca_v3.1$ currents (maximal concentration tested 1 μM, Table 1). Application of 10 μM NNC 55-0396, a T-type calcium channel inhibitor, inhibited $hCa_v3.2$ currents by 96 ± 3% (n = 5). Furthermore, Z160/NP118809 inhibited hERG channels with an IC_{50} of 7.4 μM (Zamponi et al., 2009) whereas 100 μM MONIRO-1 did not inhibit hERG channel-mediated K^+ currents (Table 1). Table 1 compares the IC_{50} values obtained for MONIRO-1 inhibition of L-, P/Q-, N-, R- and T-type calcium channels and the hERG potassium channel, with that of the control compounds, Z160/NP118809 and NNC 55-0396, and other known N- and T-type calcium channel inhibitors where electrophysiology data was obtained across a large portion of the voltage-gated calcium channel subtypes.

The current inhibition properties varied between the different MONIRO-1-sensitive Ca_v subtypes, so we analysed the interaction between MONIRO-1 and T-type ($Ca_v3.1$) and N-type ($Ca_v2.2$) calcium channels.

3.2 Differential modulation of N- and T-type calcium channels: dependence on frequency and holding potential.

We examined the inhibitory characteristics of MONIRO-1 at different test pulse durations and frequencies on $Ca_v2.2$ (Fig. 4A-B) and $Ca_v3.1$ (Fig. 5A-B), as representatives of the VGCC types targeted by MONIRO-1. $Ca_v2.2$ currents in response to shorter (45 ms) depolarizations were 1.5-times more sensitive to MONIRO-1 inhibition than those elicited by a longer (135 ms) pulse. Channels held

open by the longer pulse also recovered more completely from block (82 ± 9%, n = 5) than those briefly opened (45 ms; 47 ± 3%, n = 5) (Fig. 4A). In agreement with these findings, higher frequency stimulation of $Ca_v2.2$ channels rendered a population of channels that was more potently inhibited by MONIRO-1 (0.03, 0.1 and 0.2 Hz; Fig. 4B). At a frequency of 0.2 Hz, MONIRO-1 inhibited $Ca_v2.2$ current by 29 ± 1% (n = 5), whereas at 0.1 and 0.03 Hz, only 21 ± 1% (n = 5) and 16 ± 1% (n = 5) of the current amplitude was inhibited, respectively. Interestingly, the effects of MONIRO-1 on $Ca_v2.2$ channels are in marked contrast to its effects on $Ca_v3.1$ channels (Fig. 5A-B). In the case of $Ca_v3.1$, pulse duration did not affect $Ca_v3.1$-mediated current inhibition (% block 15 ms: 43 ± 3%, n = 5; and 50 ms: 51 ± 7%, n = 5), recovery from inhibition (% recovery 15 ms: 95 ± 1.3%, n = 5; and 50 ms: 99 ± 0.8%, n = 5) or frequency dependence of block over the same range as those tested for $Ca_v2.2$ (% block at 0.2 Hz = 43 ± 1.5%, n = 5; 0.1 Hz = 42 ± 2.3%, n = 5; and 0.03 Hz = 44 ± 1.6%, n = 5). However, at faster rates of 1 and 2 Hz, there was a significant increase in MONIRO-1 block of $Ca_v3.1$ (% block at 1 Hz = 61.0 ± 1.5%, n = 6; and 2 Hz = 71.0 ± 2.0%, n = 5). This would increase 3-fold the affinity for channels firing at faster frequencies of 2 Hz compared to those firing at rates <0.2 Hz.

To further explore the differential effects of MONIRO-1 on $Ca_v2.2$ and $Ca_v3.1$ channels, we investigated the effect of membrane holding potential on block of $Ca_v2.2$ and $Ca_v3.1$. MONIRO-1 could more effectively block $Ca_v2.2$ channels at more depolarized potentials (block at −100 mV = 34 ± 1.8%; −80 mV = 43 ± 3.2%; and −60 mV = 77 ± 5.5%, n = 5). In contrast, block at all of the holding potentials tested did not affect the degree by which MONIRO-1 inhibited $Ca_v3.1$ channels (block at −100 mV = 41 ± 0.5%; −80 mV = 46 ± 5.1%; and −60 mV = 43 ± 0.6%, n = 5) (Fig. 4C and 5C). This result highlights the state-dependent differences between MONIRO-1 inhibition of $Ca_v2.2$ and $Ca_v3.1$ channels.

3.3 Effects of MONIRO-1 on N- and T-type calcium channel activation, inactivation and recovery from inactivation.

To identify any effects MONIRO-1 may have on calcium current kinetics and understand the mechanisms behind the enhanced inhibition at depolarised membrane potentials, we examined its effects at half-maximal concentrations on $Ca_v2.2$ and $Ca_v3.1$ activation and SSI (Fig. 4D and 5D). Exposure to MONIRO-1 did not affect

the voltage-dependence of activation of $Ca_v2.2$ (control $V_{0.5}$ = 12.5 ± 0.5 mV, n = 5; MONIRO-1 $V_{0.5}$ = 12.4 ± 0.4 mV, n = 5, respectively) or $Ca_v3.1$ (control $V_{0.5\ act}$ = −34.0 ± 0.4 mV, n = 7; MONIRO-1 $V_{0.5act}$ = −34.4 ± 0.6 mV, n = 7) (Table 2). However, there was a significant ~10 mV hyperpolarizing shift in $Ca_v2.2$ SSI (control $V_{0.5\ inact}$ = −41.3 ± 0.7 mV, n = 5; MONIRO-1 $V_{0.5\ inact}$ = −52.9 ± 1.3 mV, n = 5; $P < 0.05$). An apparent decrease in the voltage-dependence of SSI was also seen (control slope factor, 5.3 ± 0.6, n = 5; MONIRO-1 slope factor, 10.2 ± 1.2, n = 5; $P < 0.05$). However, no significant changes were observed in $Ca_v3.1$ SSI in the presence of MONIRO-1 (control $V_{0.5\ inact}$ = −53.5 ± 0.6 mV, n = 6; MONIRO-1 $V_{0.5\ inact}$ = −55.1 ± 0.6 mV, n = 6) or voltage-dependence of SSI (control slope factor, 4.4 ± 0.6, n = 6; MONIRO-1 slope factor, 6.1 ± 0.5, n = 6). Channel activation and inactivation time constants were examined in the absence and presence of MONIRO-1 on $Ca_v2.2$ (30 μM) and $Ca_v3.1$ (3 μM). MONIRO-1 has no effect on either the activation or inactivation time constants of $Ca_v2.2$ (Table 2). However, MONIRO-1 application increased both activation (control: 1.90 ± 0.08 ms, n = 5; MONIRO-1: 3.45 ± 0.51 ms, n = 5: $P < 0.05$) and inactivation time constants (control: 10.78 ± 0.52 ms, n = 5; MONIRO-1: 17.91 ± 0.74 ms, n = 5, $P < 0.5$) (Table 2).

Finally, we investigated the effect of MONIRO-1 on $Ca_v2.2$ and $Ca_v3.1$ channel recovery from inactivation. MONIRO-1 had no observed effect on $Ca_v2.2$ recovery from inactivation time constants or their relative contribution to either time constants (control τ_{fast} = 0.22 ± 0.1 s, A_{fast} = 57 ± 8.5%; τ_{slow} = 2.8 ± 0.7 s, A_{slow} = 45 ± 8.6%; MONIRO-1 τ_{fast} = 0.14 ± 0.1 s, A_{fast} = 43 ± 7.0%; τ_{slow} = 2.4 ± 0.4 s, A_{slow} = 58 ± 6.2%, n = 5 respectively). However, MONIRO-1 slowed $Ca_v3.1$ recovery from inactivation by decreasing the relative contribution of the fast recovery time constant while increasing the contribution of the slow time constant (control τ_{fast} = 0.051 ± 0.008s, A_{fast} = 80.1 ± 5.1%; τ_{slow} = 0.20 ± 0.11 s, A_{slow} = 21.8 ± 5.4%; MONIRO-1 τ_{fast} = 0.026 ± 0.007s, A_{fast} = 29.6 ± 4.2%; τ_{slow} = 0.33 ± 0.03s, A_{slow} = 70 ± 4.1%, n = 6; $P < 0.05$). Therefore, MONIRO-1 can inhibit $Ca_v3.1$ more efficiently at firing frequencies > 1 Hz (Fig. 5B), as indicated by the slowed recovery from inactivation and frequency dependence, such as those prevailing in hyperexcitable neurons (Cain et al., 2010).

3. DISCUSSION

In this study, we examined the effects of an *ortho*-phenoxyanilide on the inhibition and biophysical properties of VGCCs. This *ortho*-phenoxyanilide, MONIRO-1, is a low molecular weight compound and was selected for its ability to inhibit VGCCs in a high-throughput calcium influx assay (Gleeson et al., 2015). To ascertain its selectivity and mode of action, we examined its potency of block and biophysical properties on a variety of VGCCs. MONIRO-1 was shown to be a N- and T-type calcium channel inhibitor with advantageous biophysical properties, including state- and use-dependence. It specifically targets $Ca_v3.2$ and $Ca_v2.2$, which have been implicated in various pain pathways, and $Ca_v3.1$, which is involved in cell signalling and epilepsy (Choi, 2013; Waxman et al., 2014).

Given that MONIRO-1 inhibits depolarization-activated calcium responses from SH-SY5Y cells (Gleeson et al., 2015), we determined its efficacy and selectivity against several VGCCs expressed in HEK293 cells. After screening representative members of each voltage-gated calcium channel family (L-, N-, P/Q-, R- and T-types), we established that MONIRO-1 preferentially inhibits T-type channels ($Ca_v3.1$, $Ca_v3.2$ and $Ca_v3.3$ channels), modestly interacts with N-type $Ca_v2.2$ channels (with 5–20 times less affinity compared to T-type calcium channels), and has poor efficacy for L-type ($Ca_v1.2$ and $Ca_v1.3$ channels IC_{50} > 100 μM). No other VGCCs investigated (P/Q-type $Ca_v2.1$; R-type $Ca_v2.3$) responded to high concentrations of MONIRO-1. hERG, a typical off-target channel of small molecules was not modulated by MONIRO-1 at concentrations up to 100 μM. Subsequently, we characterized the mechanism of MONIRO-1 inhibition on its primary targets, N- and T-type calcium channels.

In the present study, MONIRO-1 inhibited $Ca_v3.1$ with an IC_{50} of 3 μM, so we examined the mechanistic details of this inhibition. Many T-type calcium channel inhibitors have been identified in assays looking for inactivation state-dependent inhibitors. These studies have led to compounds that predominantly bind and alter steady-state inactivation, including TTA-A2, A-1048400 and NNC 55-0396, unlike MONIRO-1, which does not affect steady-state inactivation of $Ca_v3.1$. MONIRO-1 (3 μM) significantly slowed down both channel activation and inactivation kinetics without discernible effects of MONIRO-1 on both $V_{0.5act}$ and $V_{0.5inact}$. MONIRO-1

slowed recovery of $Ca_v3.1$ from inactivation at rates >1 Hz which was reflected as an increase in current inhibition at 1 and 2 Hz (Figure 5B,E) suggesting that MONIRO-1 would preferentially target epileptic firing neurons over normal firing neurons. Taken together, the lack of effect of MONIRO-1 on other biophysical properties examined, including the lack of effect of holding potential, suggests that it acts by binding to prevent $Ca_v3.1$ channels from transitioning from a non-conducting state to the open state. Therefore, the prolonged recovery from inactivation caused by MONIRO-1 inhibition of $Ca_v3.1$-mediated currents is likely due to the slower dissociation of the compound from the open-blocked channels, or due to it accelerating channel transitions into a slow inactivated channel conformation. A similar phenomenon has been observed for mibefradil inhibition of $Ca_v2.1$ channels (Timin et al., 2004).

$Ca_v3.1$ channels are key players in the circuitry involved in sleep including the reticular thalamic nucleus, thalamic relay neurons and neocortical pyramidal cells (Chen et al., 2014). $Ca_v3.1$ channels are highly expressed in thalamocortical neurons (Kim et al., 2001; Song et al., 2004), where they initiate entry of these neurons into bursting mode – a typical activity mode in absence seizures (Cain et al., 2013). Consequently, $Ca_v3.1$ has been directly linked to absence epilepsies (Kim et al., 2001). Disease mutations in $Ca_v3.2$ have also been linked to both rat models and human idiopathic generalized epilepsy (Khosravani et al., 2005; Powell et al., 2009) suggesting that inhibitors of both $Ca_v3.1$ and $Ca_v3.2$ could decrease neuronal firing induced by hyperactivity of these channels during epilepsy. Compound Z944, which has higher affinity for the inactivated state of T-type calcium channels over the resting state, reduced seizure activity in terms of time spent in seizure and the total number of seizures per hour (Tringham et al., 2012). During burst firing, VGCCs repetitively open and close at frequencies of 5-10 Hz (Cain et al., 2010). Ideally, an anti-epileptogenic drug targeting $Ca_v3.1$ or $Ca_v3.2$ channels in epileptogenic foci, that is, on neurons in bursting mode where the channels are in the open state. Our results suggest that MONIRO-1 modulates $Ca_v3.1$ channels by holding the channel in a non-conducting state thus prolonging recovery from inactivation, which makes the compound well suited for the study and/or potentially for the amelioration of $Ca_v3.1$ or $Ca_v3.2$-mediated epileptogenesis in neurons entering bursting mode.

Considerable research into pain physiology has focused on voltage-gated N- and T-type calcium channels. $Ca_v3.2$ channels are expressed in peripheral sensory neurons,

where they modulate pain processing by controlling dorsal root ganglion neuroexcitability (Carbone et al., 1984). $Ca_v2.2$ channels are located at presynaptic terminals in the central nervous system, where they modulate neurotransmitter release and fast synaptic transmission (Wheeler et al., 1994). MONIRO-1 inhibits $Ca_v2.2$ under resting state conditions with an IC_{50} of ~30 μM, which is approximately 10-fold higher than that observed the T-type channels. However, the effect of MONIRO-1 on $Ca_v2.2$ is enhanced at higher frequencies, where faster pacing of the channel increased inhibition. At frequencies as high as 0.2 Hz (the maximum tested), the apparent affinity increased to ~20 μM, with no observable change to the time course of activation or inactivation of the channel (Fig. 4B and Table 2).

Following this observation, we examined MONIRO-1's potential state dependence. Short (45 ms) depolarizing test pulses produced greater inhibition of $Ca_v2.2$ as well as less recovery after washout compared to a longer (135 ms) test pulse, suggesting a possible decrease in affinity for the open and/or inactivated state (Fig. 4A). MONIRO-1 had a pronounced effect on $Ca_v2.2$ channel SSI that was not paralleled in $Ca_v3.1$ (Fig. 4D) as well as strong dependence on holding potential, At −60 mV ~80% of the whole-cell current was inhibited compared to −100 mV where only ~35% of the current was blocked (Fig. 4C). Such a hyperpolarizing shift in SSI and the dependence on holding potential suggests that MONIRO-1 preferentially binds to the inactivated state of N-type calcium channels (Bean, 1984; Bean et al., 1983; Sanguinetti et al., 1984). Interestingly, unlike its effect on T-type calcium channels, MONIRO-1 did not influence N-type calcium channel recovery from inactivation (Fig. 5E) suggesting a distinct mode of action against the two channel families.

Nociceptive stimuli cause depolarization, calcium channel opening, intracellular [Ca^{2+}] increase and neuronal hyper-excitability evidenced by faster firing rates (Winquist et al., 2005). Nociceptive stimuli reduce the effective open time and increase the frequency of channel opening (Winquist et al., 2005). Sustained neuronal firing in pain syndromes increases cytosolic calcium levels in the dorsal horn and shifts calcium channels into the inactivated state. Therefore, drugs that target $Ca_v2.2$ are best suited to 'prefer' those in the inactivated state (predominant in pain syndromes), allowing normal neurotransmitter release signalled by these channels in neurons not in a pain state.

A few compounds have recently reported to exhibit use- and/or state-dependent inhibition of calcium channels involved in pain signalling, including A-1048400 (Scott et al., 2012) (compound **3**, Fig. 1), Z160/NP118809 **1** (Zamponi et al., 2009), and TROX-1 (Abbadie et al., 2010). To explore MONIRO-1 inhibitory mechanism of $Ca_v2.2$, we examined stimulation conditions comparable with those occurring in the physiological setting. Given that $Ca_v2.2$ channels can potentially accumulate in the inactivated state in hyperactive pain state conditions (Winquist et al., 2005), the selective effect of MONIRO-1 on channels in this state could be a valuable pharmacological property that would enable therapeutic targeting during neuropathic pain treatment. Frequency dependence and preference of MONIRO-1 for the inactivated $Ca_v2.2$, suggest that it or related compounds may prove useful in the prevention of high-frequency firing episodes, an important signalling mode occurring during pain transmission. Therefore, MONIRO-1 may preferentially inhibit channels in hyperexcitable states in pain-specific loci, leaving normally firing neurons unaffected (Liao et al., 2011).

4. CONCLUSION

We identified MONIRO-1 as a low molecular weight voltage-gated calcium channel antagonist with 10−100-fold higher affinity for $Ca_v3.1$, $Ca_v3.2$, $Ca_v3.3$ and $Ca_v2.2$ than other classes of VGCCs examined. MONIRO-1 is a valuable tool for the study of VGCCs because it inhibits N- and T-type calcium channels through distinct mechanisms. Given its state- and use-dependent inhibition of $Ca_v2.2$ (preferentially inhibits the inactivated state) and $Ca_v3.1$ (prohibiting channel transitions to the open state), while exhibiting frequency dependent block of both channels. MONIRO-1 is a novel lead compound that could be used to develop Ca_v channel blockers to treat VGCC pathologies, including neuropathic pain and epilepsy. MONIRO-1 shows a novel mechanism of block of hCav3.1 compared to previously described T-type calcium channel blockers, in that it slows channel activation and inactivation kinetics and traps channels at high frequency firing (>1 hZ) from transitioning to the open state while not altering steady-state inactivation. Prior to *in vivo* assessment of their analgesic potential, MONIRO-1 and analogues need to be characterised at other voltage-gated ion channels in pain pathways, including $Na_v1.7$ and $Na_v1.8$.

AUTHOR CONTRIBUTIONS

JRM, PJD, KLT and DJA designed the experiments,

JRM, LM, ECG and SS performed the experiments, JRM analysed the electrophysiological data,

JRM, PJD, KLT, and DJA prepared the figures,

JRM wrote the manuscript,

JRM, RJL, PJD, KLT, and DJA revised the manuscript.

All authors reviewed the manuscript.

ACKNOWLEDGEMENTS

We thank Dr J. E. Graham for helping with chemical synthesis and Dr. R. K. Finol-Urdaneta for providing valuable comments on drafts of the manuscript. This work was funded by a National Health and Medical Research Council Program Grant (NHMRC) awarded to D.J.A and R.J.L (APP1072113). The Monash–CSIRO Collaborative Research Support Scheme and CSIRO's Australian Biotech Growth Partnerships Theme also helped to fund this research. D.J.A is an Australian Research Council (ARC) Australian Professorial Fellow (DP1093115).

CONFLICT OF INTEREST

The authors declare that they have no conflict of interest.

REFERENCES

Abbadie C, McManus OB, Sun S-Y, Bugianesi RM, Dai G, Haedo RJ*, et al.* (2010). Analgesic effects of a substituted N-triazole oxindole (TROX-1), a state-dependent, voltage-gated calcium channel 2 blocker. Journal of Pharmacology and Experimental Therapeutics 334**:** 545-555.

Altier C, & Zamponi GW (2004). Targeting Ca^{2+} channels to treat pain: T-type versus N-type. Trends Pharmacol Sci 25**:** 465-470.

Andersson A, Baell JB, Duggan PJ, Graham JE, Lewis RJ, Lumsden NG*, et al.* (2009). Omega-conotoxin GVIA mimetics based on an anthranilamide core: effect of variation in ammonium side chain lengths and incorporation of fluorine. Bioorg Med Chem 17**:** 6659-6670.

Baell JB, Duggan PJ, Forsyth SA, Lewis RJ, Lok YP, & Schroeder CI (2004). Synthesis and biological evaluation of nonpeptide mimetics of omega-conotoxin GVIA. Bioorg Med Chem 12**:** 4025-4037.

Baell JB, Duggan PJ, Forsyth SA, Lewis RJ, Lok YP, Schroeder CI*, et al.* (2006). Synthesis and biological evaluation of anthranilamide-based non-peptide mimetics of ω-conotoxin GVIA. Tetrahedron 62**:** 7284-7292.

Bean BP (1984). Nitrendipine block of cardiac calcium channels: high-affinity binding to the inactivated state. Proc Natl Acad Sci U S A 81**:** 6388-6392.

Bean BP, Cohen CJ, & Tsien RW (1983). Lidocaine block of cardiac sodium channels. J Gen Physiol 81**:** 613-642.

Bladen C, McDaniel SW, Gadotti VM, Petrov RR, Berger ND, Diaz P*, et al.* (2015). Characterization of novel cannabinoid based T-type calcium channel blockers with analgesic effects. ACS Chem Neurosci 6**:** 277-287.

Bourinet E, Alloui A, Monteil A, Barrere C, Couette B, Poirot O*, et al.* (2005). Silencing of the Cav3.2 T-type calcium channel gene in sensory neurons demonstrates its major role in nociception. EMBO J 24**:** 315-324.

Bourinet E, Altier C, Hildebrand ME, Trang T, Salter MW, & Zamponi GW (2014). Calcium-permeable ion channels in pain signaling. Physiol Rev 94**:** 81-140.

Butterworth JFIV, & Strichartz GR (1990). Molecular mechanisms of local anesthesia: a review. Anesthesiology 72**:** 711-734.

Cain SM, & Snutch TP (2010). Contributions of T-type calcium channel isoforms to neuronal firing. Channels 4**:** 475-482.

Cain SM, & Snutch TP (2013). T-type calcium channels in burst-firing, network synchrony, and epilepsy. Biochimica et Biophysica Acta (BBA) - Biomembranes 1828**:** 1572-1578.

Carbone E, & Lux HD (1984). A low voltage-activated, fully inactivating Ca channel in vertebrate sensory neurones. Nature 310**:** 501-502.

Catterall WA, Perez-Reyes E, Snutch TP, & Striessnig J (2005). International union of pharmacology. XLVIII. Nomenclature and structure-function relationships of voltage-gated calcium channels. Pharmacol Rev 57**:** 411-425.

Chen Y, Chen Y, Parker WD, & Wang K (2014). The role of T-type calcium channel genes in absence seizures. Front Neurol 5**:** 1-8.

Cheong E, & Shin H-S (2013). T-type Ca^{2+} channels in normal and abnormal brain functions. Physiol Rev 93**:** 961-992.

Choi K-H (2013). The design and discovery of T-type calcium channel inhibitors for the treatment of central nervous system disorders. Expert Opin Drug Discov 8**:** 919-931.

Choi S, Na HS, Kim J, Lee J, Lee S, Kim D*, et al.* (2007). Attenuated pain responses in mice lacking $Ca_v3.2$ T-type channels. Genes Brain Behav 6**:** 425-431.

Chouabe C, Drici M-D, Romey G, Barhanin J, & Lazdunski M (1998). HERG and KvLQT1/IsK, the Cardiac K^+ Channels Involved in Long QT Syndromes, Are Targets for Calcium Channel Blockers. Mol Pharmacol 54**:** 695-703.

Dai G, Haedo RJ, Warren VA, Ratliff KS, Bugianesi RM, Rush A*, et al.* (2008). A high-throughput assay for evaluating state dependence and subtype selectivity of Ca_v2 calcium channel inhibitors. Assay Drug Dev Technol 6**:** 195-212.

Duggan PJ, Lewis RJ, Phei Lok Y, Lumsden NG, Tuck KL, & Yang A (2009). Low molecular weight non-peptide mimics of omega-conotoxin GVIA. Bioorg Med Chem Lett 19**:** 2763-2765.

Eller P, Berjukov S, Wanner S, Huber I, Hering S, Knaus HG*, et al.* (2000). High affinity interaction of mibefradil with voltage-gated calcium and sodium channels. Br J Pharmacol 130**:** 669-677.

Flatters SJL, & Bennett GJ (2004). Ethosuximide reverses paclitaxel- and vincristine-induced painful peripheral neuropathy. Pain 109**:** 150-161.

Francois A, Kerckhove N, Meleine M, Alloui A, Barrere C, Gelot A*, et al.* (2013). State-dependent properties of a new T-type calcium channel blocker enhance $Ca_V3.2$ selectivity and support analgesic effects. Pain 154**:** 283-293.

François A, Laffray S, Pizzoccaro A, Eschalier A, & Bourinet E (2014). T-type calcium channels in chronic pain: Mouse models and specific blockers. Pflugers Arch - Eur J Physiol 466**:** 707-717.

Gleeson EC, Graham JE, Spiller SS, Vetter I, Lewis RJ, Duggan PJ*, et al.* (2015). Inhibition of N-Type calcium channels by fluorophenoxyanilide derivatives. Mar Drugs 13**:** 2030.

Gold MS, & Gebhart GF (2010). Nociceptor sensitization in pain pathogenesis. Nat Med 16**:** 1248-1257.

Gomora JC, Murbartian J, Arias JM, Lee JH, & Perez-Reyes E (2002). Cloning and expression of the human T-type channel Ca(v)3.3: insights into prepulse facilitation. Biophys J 83**:** 229-241.

Guo D, & Hu J (2014). Spinal presynaptic inhibition in pain control. Neuroscience 283**:** 95-106.

Hondeghem LM, & Katzung BG (1984). Antiarrhythmic agents: the modulated receptor mechanism of action of sodium and calcium channel-blocking drugs. Annu Rev Pharmacol Toxicol 24**:** 387-423.

Khosravani H, Bladen C, Parker DB, Snutch TP, McRory JE, & Zamponi GW (2005). Effects of Cav3.2 channel mutations linked to idiopathic generalized epilepsy. Ann Neurol 57**:** 745-749.

Kim D, Song I, Keum S, Lee T, Jeong M-J, Kim S-S*, et al.* (2001). Lack of the burst firing of thalamocortical relay neurons and resistance to absence seizures in mice lacking α1G T-Type Ca^{2+} channels. Neuron 31**:** 35-45.

Kraus RL, Li Y, Gregan Y, Gotter AL, Uebele VN, Fox SV*, et al.* (2010). In vitro characterization of T-type calcium channel antagonist TTA-A2 and in vivo effects on arousal in mice. Journal of Pharmacology and Experimental Therapeutics 335**:** 409-417.

Lee MS (2014). Chapter Four - Recent progress in the discovery and development of N-type calcium channel modulators for the treatment of pain. In Prog Med Chem. eds Lawton G., & Witty D.R. Elsevier, pp 147-186.

Lee S (2013). Pharmacological inhibition of voltage-gated Ca^{2+} channels for chronic pain relief. Curr Neuropharm 11**:** 606-620.

Liao Y-F, Tsai M-L, Chen C-C, & Yen C-T (2011). Involvement of the $Ca_v3.2$ T-type calcium channel in thalamic neuron discharge patterns. Mol Pain 7**:** 43.

Matthews EA, & Dickenson AH (2001). Effects of ethosuximide, a T-type Ca2+ channel blocker, on dorsal horn neuronal responses in rats. Eur J Pharmacol 415**:** 141-149.

McCleskey EW, Fox AP, Feldman DH, Cruz LJ, Olivera BM, Tsien RW*, et al.* (1987). Omega-conotoxin: direct and persistent blockade of specific types of calcium channels in neurons but not muscle. Proc Natl Acad Sci U S A 84**:** 4327-4331.

Nilius B, Prenen J, Voets T, Eggermont J, & Droogmans G (1998). Activation of volume-regulated chloride currents by reduction of intracellular ionic strength in bovine endothelial cells. The Journal of Physiology 506**:** 353-361.

Perret D, & Luo ZD (2009). Targeting voltage-gated calcium channels for neuropathic pain management. Neurotherapeutics 6**:** 679-692.

Pope JE, & Deer TR (2013). Ziconotide: a clinical update and pharmacologic review. Expert Opin Pharmacother 14**:** 957-966.

Powell KL, Cain SM, Ng C, Sirdesai S, David LS, Kyi M*, et al.* (2009). A Cav3.2 T-type calcium channel point mutation has splice-variant-specific effects on function and segregates with seizure expression in a polygenic rat model of absence epilepsy. J Neurosci 29**:** 371-380.

Reger TS, Yang Z-Q, Schlegel K-AS, Shu Y, Mattern C, Cube R*, et al.* (2011). Pyridyl amides as potent inhibitors of T-type calcium channels. Bioorg Med Chem Lett 21**:** 1692-1696.

Saegusa H, Kurihara T, Zong S, Kazuno A-A, Matsuda Y, Nonaka T*, et al.* (2001). Suppression of inflammatory and neuropathic pain symptoms in mice lacking the N-type Ca^{2+} channel. EMBO Journal 20**:** 2349-2356.

Sanguinetti MC, & Kass RS (1984). Voltage-dependent block of calcium channel current in the calf cardiac Purkinje fiber by dihydropyridine calcium channel antagonists. Circ Res 55**:** 336-348.

Scott VE, Vortherms TA, Niforatos W, Swensen AM, Neelands T, Milicic I*, et al.* (2012). A-1048400 is a novel, orally active, state-dependent neuronal calcium channel blocker that produces dose-dependent antinociception without altering hemodynamic function in rats. Biochem Pharmacol 83**:** 406-418.

Sekiguchi F, & Kawabata A (2013). T-type calcium channels: functional regulation and implication in pain signaling. J Pharmacol Sci 122**:** 244-250.

Simms BA, & Zamponi GW (2014). Neuronal voltage-gated calcium channels: structure, function, and dysfunction. Neuron 82**:** 24-45.

Song I, Kim D, Choi S, Sun M, Kim Y, & Shin H-S (2004). Role of the α1G T-type calcium channel in spontaneous absence seizures in mutant mice. Journal of Neuroscience 24**:** 5249-5257.

Swensen AM, Herrington J, Bugianesi RM, Dai G, Haedo RJ, Ratliff KS*, et al.* (2012). Characterization of the substituted N-triazole oxindole TROX-1, a small-molecule, state-dependent inhibitor of Ca(V)2 calcium channels. Mol Pharmacol 81**:** 488-497.

Timin E, Berjukow S, & Hering S (2004). Concepts of state-dependent pharmacology of calcium channels. In Calcium Channel Pharmacology. ed McDonough S. Springer US, pp 1-19.

Todorovic SM, Meyenburg A, & Jevtovic-Todorovic V (2002). Mechanical and thermal antinociception in rats following systemic administration of mibefradil, a T-type calcium channel blocker. Brain Res 951**:** 336-340.

Tranberg CE, Yang A, Vetter I, McArthur JR, Baell JB, Lewis RJ*, et al.* (2012). ω-Conotoxin GVIA mimetics that bind and inhibit neuronal $Ca_v2.2$ ion channels. Mar Drugs 10**:** 2349-2368.

Tringham E, Powell KL, Cain SM, Kuplast K, Mezeyova J, Weerapura M*, et al.* (2012). T-type calcium channel blockers that attenuate thalamic burst firing and suppress absence seizures. Sci Transl Med 4**:** 121ra119.

Wang F, Yan Z, Liu Z, Wang S, Wu Q, Yu S*, et al.* (2016). Molecular basis of toxicity of N-type calcium channel inhibitor MVIIA. Neuropharmacology 101**:** 137-145.

Waxman SG, & Zamponi GW (2014). Regulating excitability of peripheral afferents: emerging ion channel targets. Nat Neurosci 17**:** 153-163.

Wen XJ, Xu SY, Chen ZX, Yang CX, Liang H, & Li H (2010). The roles of T-type calcium channel in the development of neuropathic pain following chronic compression of rat dorsal root ganglia. Pharmacology 85**:** 295-300.

Wheeler DB, Randall A, & Tsien RW (1994). Roles of N-type and Q-type Ca^{2+} channels in supporting hippocampal synaptic transmission. Science 264**:** 107-111.

Winquist RJ, Pan JQ, & Gribkoff VK (2005). Use-dependent blockade of Cav2.2 voltage-gated calcium channels for neuropathic pain. Biochem Pharmacol 70**:** 489-499.

Zamponi GW, Feng Z-P, Zhang L, Pajouhesh H, Ding Y, Belardetti F*, et al.* (2009). Scaffold-based design and synthesis of potent N-type calcium channel blockers. Bioorg Med Chem Lett 19**:** 6467-6472.

Zikolova S, & Ninov K (1972). Analogs of N^1-benzhydryl-N^4-cinnamylpiperazine (cinnarizine). II. N^1-Substituted-N^4-benzhydrylpiperazines. Tr Nauchnoizsled Khim-Farm Inst 8**:** 59-67.

FIGURE LEGENDS

Figure 1. Chemical structures of compounds **1** (Z160/NP118809), **2** (MONIRO-1) and **3** (NNC 55-0396) relevant to this study.

Figure 2. MONIRO-1 inhibition of human $Ca_v2.2$- and $Ca_v3.1$-mediated currents in HEK293 cells. **A**. Superimposed whole-cell Ca^{2+} currents recorded from HEK293 cells stably expressing human N-type calcium ($hCa_v2.2$) channels ($\alpha_{1B} + \beta3 + \alpha2\delta1$) in response to depolarizing pulses (135 ms duration) to +20 mV from a holding potential of −80 mV. Representative current traces obtained in the absence (a) and presence of 50 (b) and 100 μM (d) MONIRO-1, and after respective washouts (c, e). **B**. Peak inward Ca^{2+} current amplitude plotted as a function of time. Time course of inhibition and current amplitude recovery in the presence and following washout of 50 and 100 μM MONIRO-1. Representative currents shown in (A) were obtained at the times indicated by the lower case letters. **C**. Superimposed whole-cell Ca^{2+} currents recorded from HEK293 cells transiently expressing human T-type calcium channel, $hCa_v3.1$. These Ca^{2+} currents are in response to depolarizing pulses (50 ms duration) to −25 mV from a holding potential of −80 mV. Representative current traces obtained in the absence (a) and presence of 10 (b) and 100 μM (c) MONIRO-1. **D**. Peak inward Ca^{2+} current amplitude plotted as a function of time. Time course of inhibition and recovery of current amplitude in the absence (a) and presence of 10 (b) and 100 μM (c) MONIRO-1.

Figure 3. MONIRO-1 inhibition of voltage-gated calcium channels. **A**. Concentration–response of MONIRO-1 at $hCa_v2.2$ (open square), $hCa_v3.1$ (open upward triangle), $hCa_v3.2$ (open circle) and $hCa_v3.3$ (open downward triangle) channels expressed in HEK293 cells. Fitted curves gave IC_{50} values of 34 ± 3.6 μM (n = 5-7 cells per concentration) towards $hCa_v2.2$; 3.3 ± 0.3 μM (n = 5-6 cells per concentration) against $hCa_v3.1$; 1.7± 0.1 μM against $hCa_v3.2$ (n = 5-9 cells per concentration); and 7.2 ± 0.3 μM (n = 5 cells per concentration) against $hCa_v3.3$. **B**. Fraction of current inhibited by 100 (solid) or 10 μM (striped) MONIRO-1 at $Ca_v1.3$, $Ca_v2.1$, $Ca_v2.2$, $Ca_v2.3$, $Ca_v3.1$ and $Ca_v3.2$ channels. Cells were held at −80 mV and pulsed at 0.1 Hz to the voltage determined to elicit the peak inward current previously determined from an I-V protocol. The number of cells is indicated in parentheses.

Figure 4. MONIRO-1 block of human $Ca_v2.2$ channels. **A. (i)** Recovery from block (striped) and (ii) fraction blocked (solid) by 30 µM MONIRO-1, with a depolarizing pulse duration of 45 ms (open bars) or 135 ms (filled bars), from a holding potential of -80mV to a test potential that elicits maximal inward current, repeated every 10 s. The number of cells is indicated in parentheses. **B.** Fraction of current inhibited by 10 µM MONIRO-1 at three different frequencies (0.03, 0.1, and 0.2 Hz; holding potential −80 mV). The number of cells is indicated in parentheses. **C.** Effect of holding potential (−100, −80 and −60 mV) on the fraction of current blocked by 30 µM MONIRO-1 (pulsed at 0.1 Hz). The number of cells is indicated in parentheses. **D.** Activation and SSI curves in the absence (control; solid symbols) and presence of 30 µM MONIRO-1 (open symbols). Activation curves were generated through indicated depolarizing test pulses (135 ms) from a holding potential of −80 mV, repeated every 10s. For SSI curves, selected prepulse potentials (−120 to 0 mV in 5 mV increments for 10 s) were applied prior to a test pulse (135 ms) determined from the peak current, repeated every 15 s from a holding potential of −80 mV. **E.** Recovery from inactivation in the absence (control; solid symbols) and presence of 30 µM MONIRO-1 (open symbols). A two-pulse protocol (Inset) was repeated every 15 s, where the time was varied between the first fully inactivating pulse and the test pulse (0-10 s). * $P<0.05$ and n.s.= not statistically significant, based on student's t-test.

Figure 5. MONIRO-1 block of human $Ca_v3.1$ channels. **A. (i)** Bar graph showing recovery from block (striped) and (ii) fraction blocked (solid) by 3 µM MONIRO-1, with a depolarizing pulse duration of 15 ms (open bars) or 50 ms (filled bars), from a holding potential of −80mV repeated every 10 s. The number of cells is indicated in parentheses. **B.** Bar graph of the fractional current inhibited by 3 µM MONIRO-1 at five different frequencies (0.03, 0.1, 0.2, 1 and 2 Hz; holding potential −80 mV). The number of cells is indicated in parentheses. **C.** Effect of holding potential (−100, −80 and −60 mV) on the fraction of current inhibited by 3 µM MONIRO-1 (pulsed at 0.1 Hz). The number of cells is indicated in parentheses. **D.** Activation and SSI curves in the absence (control; solid symbols) and presence of 3 µM MONIRO-1 (open symbols). Activation curves were generated through indicated depolarizing test pulses (50 ms) from a holding potential of −80 mV, repeated every 10s. For SSI curves, selected prepulse potential values (-85 to -20 mV in 5mV increments for 1 s) were applied prior to a test pulse (50 ms) determined from the peak

current, repeated every 10 s from a holding potential of −80 mV. **E.** Recovery from inactivation in the absence (control; solid symbols) and presence of 3 μM MONIRO-1 (open symbols). A two-pulse protocol (Inset) was repeated every 15 s, where the time was varied between the first fully inactivating pulse and the test pulse. * $P<0.05$ and n.s.= not statistically significant based on student's t-test.

Table 1. Comparison of IC_{50} values obtained for MONIRO-1 inhibition of L-, P/Q-, N-, R- and T-type calcium channels and the hERG potassium channel, with control compounds Z160/NP118809 and NNC 55-0396, and other known N- and T-type calcium channel inhibitors.

	L-type	**P/Q-type**	**N-type**	**R-type**	**T-type**	**hERG**
Z160/NP118809 (Zamponi et al., 2009)	12 μM† ($Ca_v1.2$)	–	0.28 μM*	–	–	7.4 μM
* MONIRO-1	27% @ 100 μM ($Ca_v1.3$) 46% @ 100 μM ($Ca_v1.2$)	>100 μM	34 μM	>100 μM	3.3 μM ($Ca_v3.1$) 1.7 μM ($Ca_v3.2$) 7.2 μM ($Ca_v3.3$)	>100 μM
A-1048400 (Scott et al., 2012)	28 μM	1.3 μM	0.8 μM	–	0.9 μM ($Ca_v3.2$)	–
Z944 (Tringham et al., 2012)	32 μM ($Ca_v1.2$)	–	11 μM	–	0.05 μM ($Ca_v3.1$) 0.16 μM ($Ca_v3.2$)	7.8 μM
NNC 55-0396 (Chen et al., 2014)	–	–	–	–	6.8 μM† ($Ca_v3.1$) 96% @10 μM* ($Ca_v3.2$)	–
Ziconotide (Wang et al., 2016)	–	>10 μM	0.18 μM†	–	–	–
TTA-A2 (Kraus et al., 2010)	>30 μM† ($Ca_v1.2$)	>30 μM†	>30 μM†	>30 μM†	0.09 μM ($Ca_v3.1$) 0.09 μM ($Ca_v3.2$)	–
TROX-1 (Swensen et al., 2012)	–	0.29 μM	0.19 μM	0.28 μM	–	–

*This work. †Studies were performed with HEK293 cells stably expressing the desired voltage-gated calcium channel. –, not tested.

Table 2. Comparison of activation and inactivation parameters between $Ca_v2.2$ and $Ca_v3.1$ before and after application of MONIRO-1

	$Ca_v2.2$		**$Ca_v3.1$**	
	Control	**MONIRO-1 (30 µM)$^+$**	**Control**	**MONIRO-1 (3 µM)$^+$**
tau activation	1.81 ± 0.15 ms (5)	1.51 ± 0.17 ms (5)	1.90 ± 0.08 ms (5)	3.45 ± 0.51 ms (5)*
tau inactivation	61.75 ± 13.69 ms (5)	44.45 ± 7.61 ms (5)	10.78 ± 0.52 ms (5)	17.91 ± 0.74 ms (5)*
$V_{0.5}$ activation	12.5 ± 0.5 mV (5)	12.4 ± 0.4 mV (5)	–34.0 ± 0.4 mV (7)	–34.4 ± 0.6 mV (7)
$V_{0.5}$ inactivation	–41.3 ± 0.7 mV (5)	–52.9 ± 1.3 mV (5)*	–53.5 ± 0.6 mV (6)	–55.1 ± 0.6 mV (6)
Slope factor	5.3 ± 0.6 (5)	10.2 ± 1.2 (5)*	4.4 ± 0.6 (6)	6.1 ± 0.5 (6)

*P <0.05 compared to control, students t-test.

$^+$concentration chosen based on IC_{50} of individual channel

Figure 1

1 Z160/NP118809

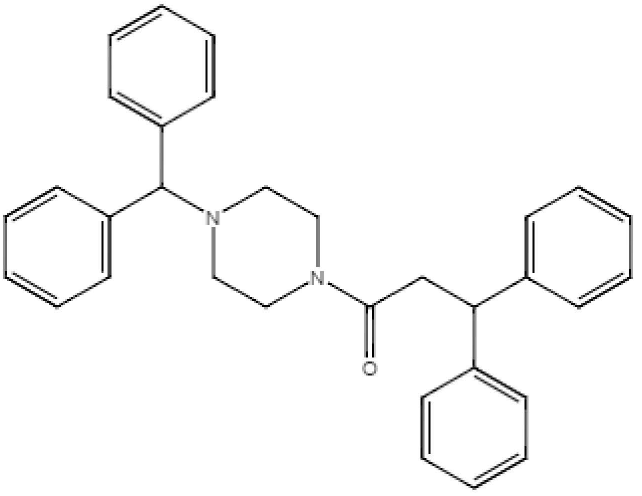

2 MONIRO-1

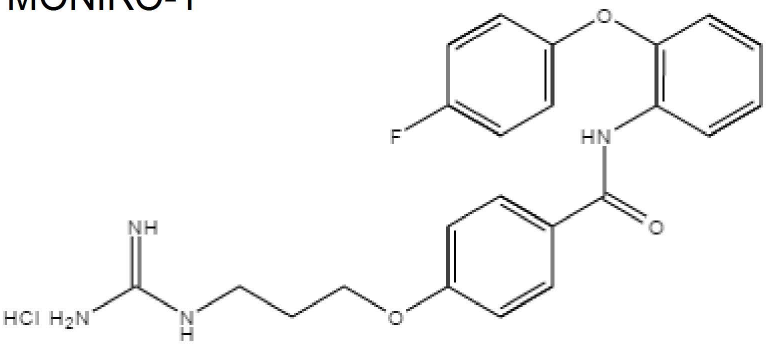

3 NNC 55-0396

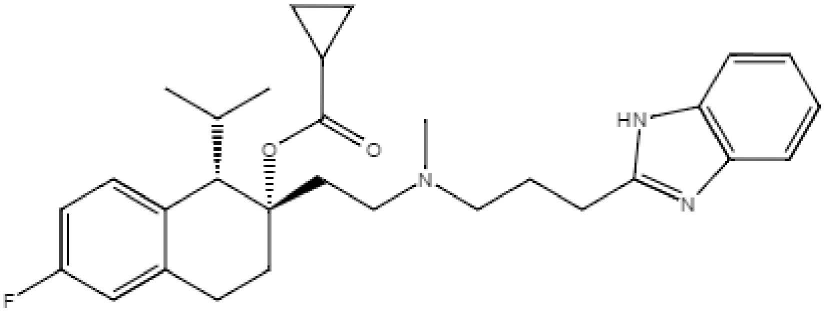

Figure 2

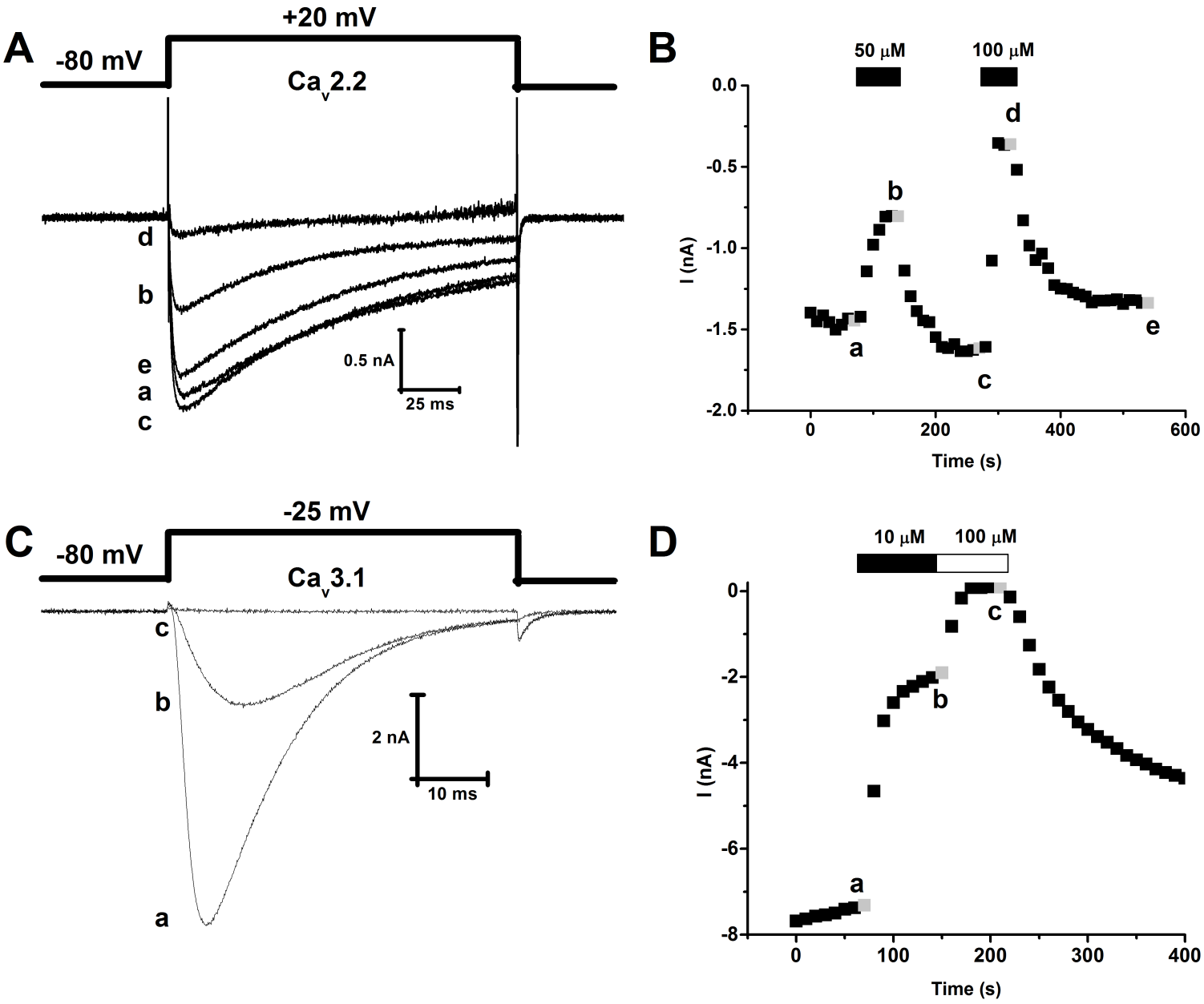
A
+20 mV
-80 mV
Cav2.2
d
b
e
a
c
0.5 nA
25 ms
B
50 μM
100 μM
d
b
a
c
e
I (nA)
Time (s)
C
-25 mV
-80 mV
Cav3.1
c
b
a
2 nA
10 ms
D
10 μM
100 μM
c
b
a
I (nA)
Time (s)

Figure 3

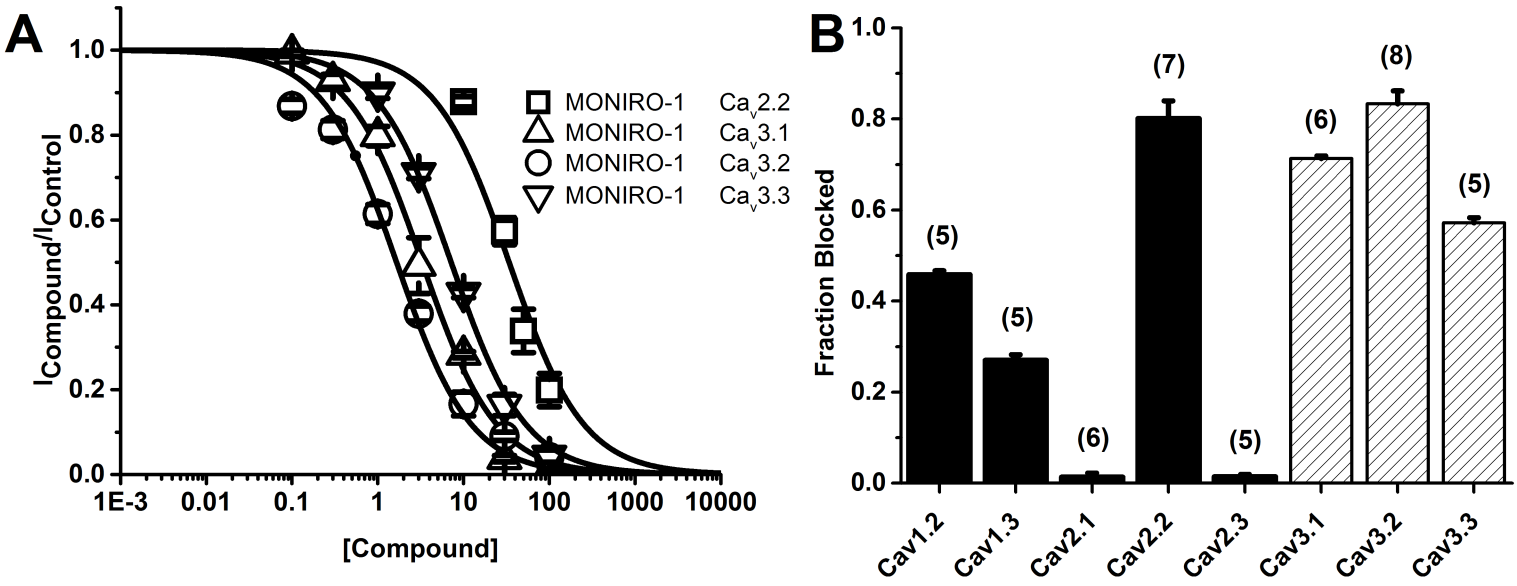
A
1.0
0.8
0.6
0.4
0.2
0.0
I Compound/I Control
1E-3
0.01
0.1
1
10
100
1000
10000
[Compound]
MONIRO-1 Cav2.2
MONIRO-1 Cav3.1
MONIRO-1 Cav3.2
MONIRO-1 Cav3.3
B
Fraction Blocked
(5)
(5)
(6)
(7)
(5)
(6)
(8)
(5)
Cav1.2
Cav1.3
Cav2.1
Cav2.2
Cav2.3
Cav3.1
Cav3.2
Cav3.3

Figure 4

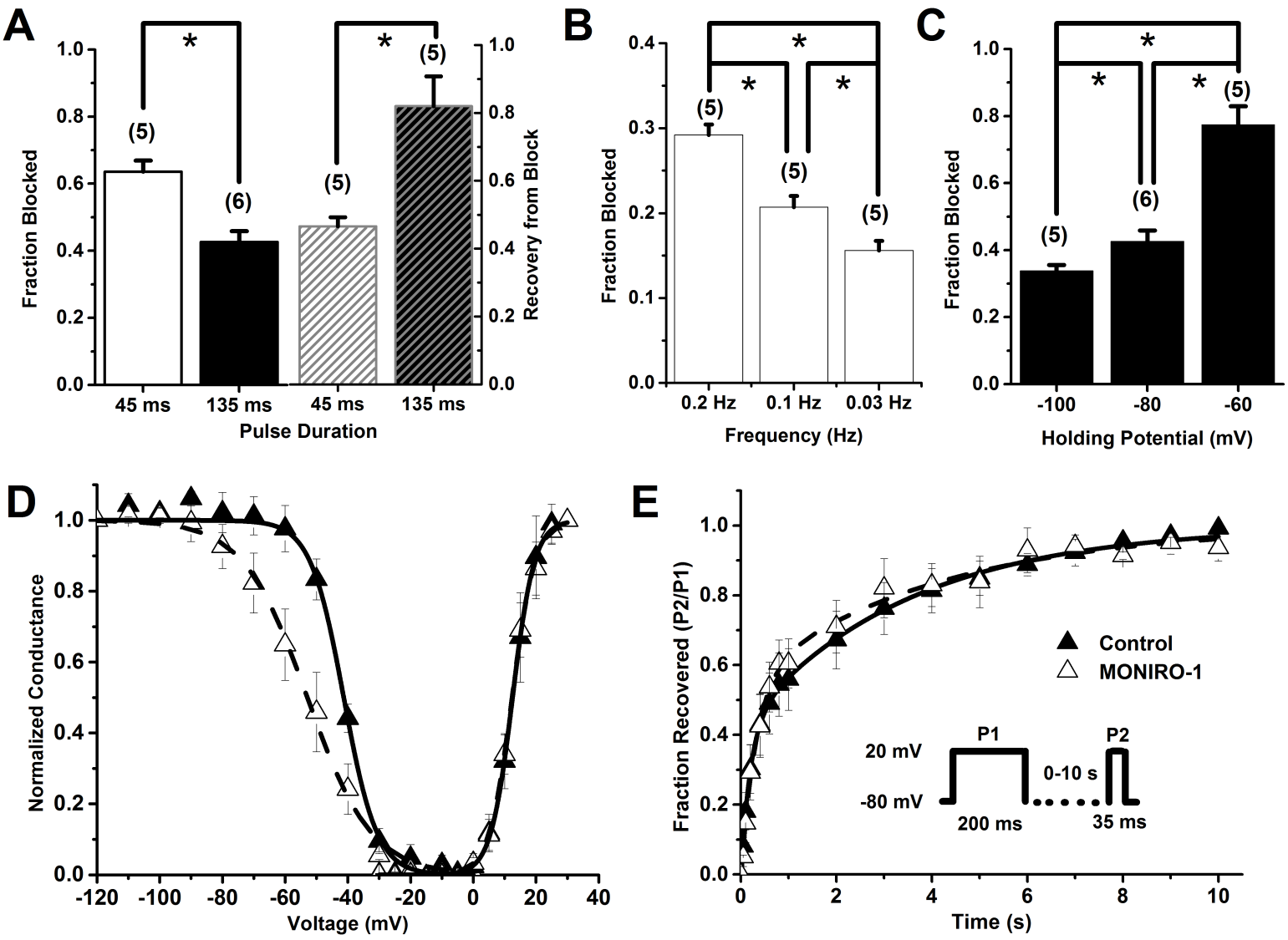
A
Fraction Blocked
Recovery from Block
(5)
(6)
(5)
(5)
*
*
45 ms
135 ms
45 ms
135 ms
Pulse Duration
B
Fraction Blocked
(5)
(5)
(5)
*
*
*
0.2 Hz
0.1 Hz
0.03 Hz
Frequency (Hz)
C
Fraction Blocked
(5)
(6)
(5)
*
*
*
-100
-80
-60
Holding Potential (mV)
D
Normalized Conductance
Voltage (mV)
E
Fraction Recovered (P2/P1)
Control
MONIRO-1
P1
P2
20 mV
-80 mV
200 ms
0-10 s
35 ms
Time (s)

Figure 5

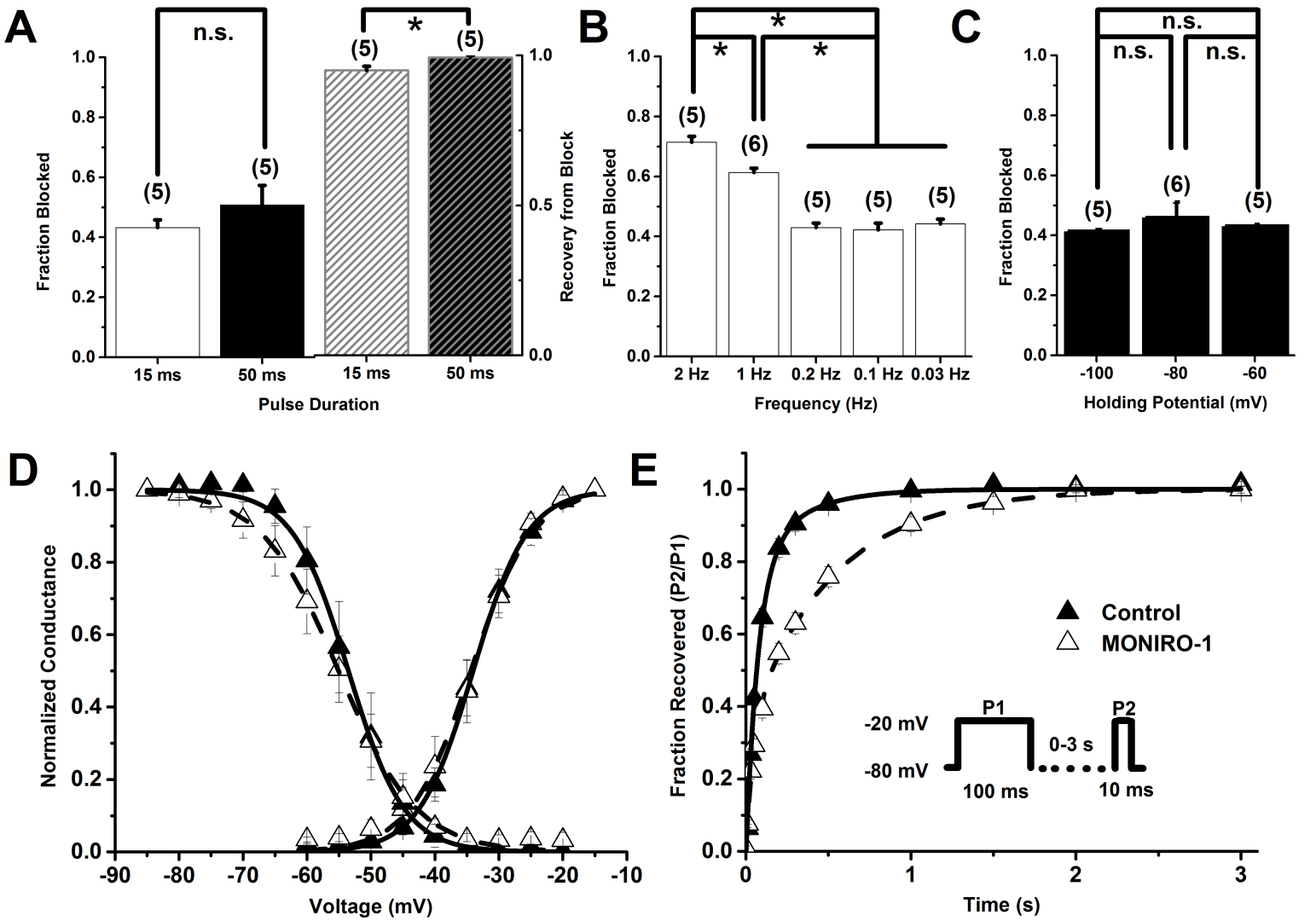
A
n.s.
*
(5)
(5)
(5)
(5)
Fraction Blocked
Recovery from Block
15 ms
50 ms
15 ms
50 ms
Pulse Duration
B
*
*
*
(5)
(6)
(5)
(5)
(5)
Fraction Blocked
2 Hz
1 Hz
0.2 Hz
0.1 Hz
0.03 Hz
Frequency (Hz)
C
n.s.
n.s.
n.s.
(5)
(6)
(5)
Fraction Blocked
-100
-80
-60
Holding Potential (mV)
D
Normalized Conductance
Voltage (mV)
E
Fraction Recovered (P2/P1)
Control
MONIRO-1
-20 mV
-80 mV
P1
P2
0-3 s
100 ms
10 ms
Time (s)